ADVANCED MATERIALS INTERFACES
Open Access
www.advmatinterfaces.de

Optimizing Atomic Layer Deposition Processes with Nanowire-Assisted TEM Analysis

Peter Schweizer, Lilian M. Vogl, Xavier Maeder, Ivo Utke, and Johann Michler*

Atomic layer deposition (ALD) is one of the premier methods to synthesize ultra-thin materials on complex surfaces. The technique allows for precise control of the thickness down to single atomic layers, while at the same time providing uniform coverage even for structures with extreme aspect ratios such as deep trenches or wires. While many materials can be readily deposited using ALD there is still a lot of research going on to make other materials more accessible. When establishing a new process or adapting an existing process to a new reactor, precise optimization of the deposition parameters is necessary. However, characterizing the parameters of deposition rate, uniformity, composition, and structure is a challenging and time-consuming task. Here a method is presented to optimize these process parameters during ALD deposition using high-aspect ratio nanowires and transmission electron microscopy (TEM). Nanowire samples are prepared directly on TEM grids that are put into the ALD reactor during deposition. Within min of the process the coated nanowires can be analyzed by TEM to obtain the thickness of the layers, chemical composition, crystallinity, and conformality of the coating. This allows for a high testing throughput and subsequently a rapid optimization of deposition parameters.

1. Introduction

Atomic layer deposition (ALD) is a widely established deposition technique that makes use of self-limiting layer-by-layer growth to deposit a thin layer of material on arbitrary substrates from the vapor phase.[1–3] Most commonly, ALD is used to deposit oxides such as aluminum oxide[4,5] or zinc oxide[6] but the deposition of other materials such as nitrides[7,8] and even metals[9,10] has been reported as well. The process parameters of ALD critically depend on characteristics of the deposition instrument like the chamber geometry and pump efficiency.[11,12] To efficiently deposit materials using ALD it is therefore important to optimize the process parameters like pulse and purge times for each instrument. In addition, using novel precursors also requires extensive characterization and calibration.[13,14] Due to the generally low deposition rates of ALD processes, it is difficult to quickly assess the growth and quality of an ALD layer easily. Established methods to characterize ALD layers after synthesis include ellipsometry, optical spectroscopy, time-of-flight secondary ion mass spectrometry (ToF-SIMS), X-ray reflectivity (XRR), atom probe tomography (APT) or transmission electron microscopy (TEM) cross sections.[15–21] Each of these methods has distinct advantages and gives information about certain aspects of deposited films. For instance, ellipsometry, and XRR can be readily employed on as-prepared films. They can measure the thickness of a deposited ALD layer but cannot analyze the chemical composition. The chemical composition can be studied, for instance, using ToF-SIMS, which may have trouble analyzing structures with a high aspect ratio, or APT, which is limited to small volumes. In contrast, TEM can give information about both the thickness and chemical composition even for high aspect-ratio structures but typically requires complex and time-consuming sample preparation like focused ion beam lift-outs[22] or conventional grinding, polishing, and ion milling.[23] Here we introduce a way of eliminating this preparation process for TEM to be able to look at depositions directly after processing while maintaining the analysis power of TEM. This enables the rapid characterization of deposited films and therefore speeds up the optimization of process parameters. To achieve this, we use nanowires grown directly on a TEM grid as a substrate which can be put into an ALD reactor during processing. Nanowires with a typical thickness of ≤100 nm are thin enough so that a deposition can be viewed in TEM directly after processing. In this study, we use metal nanowires (Cu and Au) made by a physical vapor deposition process at elevated temperatures.[24] While these wires are convenient as they can be grown directly on a TEM grid and have high quality and stability,[25] in principle all sorts of nanowires can be used as templates for the process such as semiconductors[26] or metal oxides.[27] To showcase the

P. Schweizer, L. M. Vogl, X. Maeder, I. Utke, J. Michler
Swiss Federal Laboratories for Materials Science and Engineering (Empa)
Laboratory for Mechanics of Materials and Nanostructures
Feuerwerkerstrasse 39, Thun 3602, Switzerland
E-mail: peter.schweizer@empa.ch

J. Michler
École Polytechnique Fédérale de Lausanne (EPFL)
Lausanne 1015, Switzerland

The ORCID identification number(s) for the author(s) of this article can be found under https://doi.org/10.1002/admi.202301064

DOI: 10.1002/admi.202301064

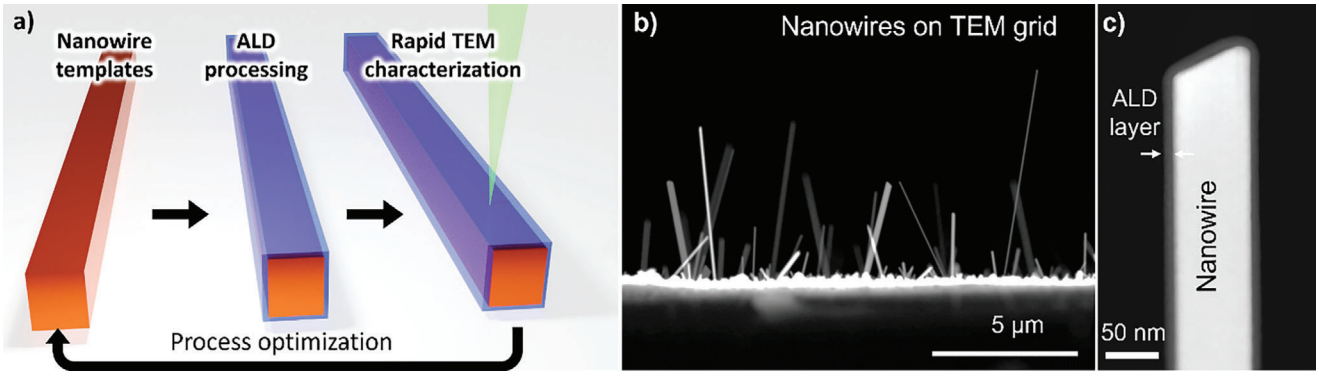

Figure 1. Overview of the process. a) Schematic representation of rapid ALD process characterization using nanowires and TEM. b) TEM overview image of metallic nanowires on a TEM grid. c) Close-up STEM image of a nanowire coated with an ALD shell.

potential of using commercial wires, we tested the deposition on solution-grown silver nanowires (see Figure S1, Supporting Information). **Figure 1a** shows the whole approach schematically: nanowires are grown directly on TEM grids or they can be transferred to grids. These grids are then put into an ALD reactor for processing. Directly after the process, the coated nanowires can be characterized using TEM to learn about the deposition rate, structure, and chemistry of the film. There is no further preparation necessary, meaning that there can be as little as 5 min between the end of the process and the first TEM results. The nanowires used in this work have a high aspect ratio (see Figure 1b for an overview image of nanowires sticking out from the side of a TEM grid), which makes them also suitable to test the conformality of the coating. In addition, the wires have a facetted cross section[28] which enables us to look along a straight edge when viewing a deposition (as shown schematically in Figure 1a). To ensure that the facets are parallel to the viewing direction we look for wires oriented in a <110> or <112> zone axis that also contains the <110> growth direction. This means that either the {111} or {200} facets are oriented edge-on. Alternatively, a wire can be tilted to one of these orientations. It is also important to select wires that do not have any surface defects to ensure an optimal analysis. An advantage of TEM is that very thin layers can be characterized, which eliminates the need to deposit thicker films and speeds up the whole optimization process. In this study, we focused on the well-established trimethylaluminum (TMA)/water process[29] to deposit aluminum oxide using ALD. Figure 1c shows a high-angle annular dark-field (HAADF) scanning transmission electron microscopy (STEM) image of a metal nanowire coated with an aluminum oxide layer. The layer corresponds to 50 ALD cycles (growth temperature of 120 °C) and has a thickness of 5 nm with the material being deposited equally on all sides of the wire. In addition to the thickness, the layers can also be analyzed regarding their chemical composition, crystallinity, and conformality detailed below.

2. Detailed TEM Characterization

TEM offers a wide variety of different techniques that enable precise characterization of the structure and properties of a deposited thin film. Here we use imaging for thickness control, energy dispersive X-ray spectroscopy (EDX) to determine the chemical composition, tilt-series to study conformality, and high-resolution imaging to assess the crystallinity and attachment to the substrate. **Figure 2** demonstrates typical results obtained from ALD layers grown on nanowires. The thickness (see Figure 2a) can be directly measured using imaging (in this case HAADF STEM imaging, however, conventional TEM can be used just the same). The accuracy of the measurement generally depends on the resolution of the instrument with modern microscopes reaching values well <1 Å.[30] However, while in this study we used an aberration-corrected instrument to achieve atomic resolution, this is not necessary for ALD process optimization. In fact, even a modern scanning electron microscope (SEM) operated in transmission mode[31,32] has a sufficiently high resolution for the here-presented procedure, in addition to the capability of EDX and even diffraction,[33] making our approach viable for many labs. Looking at the image of the ALD layer on the nanowire, we can see that it is conformal around the wire and has a low roughness. The thickness, on average, is ≈5 nm. The contrast of the ALD layer is uniform, indicating a uniform density throughout the deposition. To confirm the chemistry of the ALD layer, EDX maps were acquired (see Figure 2b). The outer layer is made of aluminum and oxygen as expected for the ALD process. In an EDX line-scan (see Figure 2c) we can see a continuous aluminum and oxygen layer around the wire with a ratio of aluminum to oxygen of 2:3, which is close to what would be expected for Al_2O_3. Going to atomic resolution (Figure 2d) we see a direct attachment of the ALD layer on the metal nanowire. While the nanowire is crystalline (face-centered cubic structure, here in a <110> zone axis) the aluminum oxide is entirely amorphous. The nanowire has a very low roughness of one to two monolayers making it an ideal substrate for this process.

In order to test the conformality of the deposited layer, a specimen can be tilted in TEM to look at it in different projections. Figure 2e shows a wire coated with a 100 nm thick ALD layer at different tilt angles. The coating looks largely uniform across all the different projections, with only a small difference in thickness that can be attributed to the curvature of the wire.

This demonstrates that the nanowire geometry is very useful for analyzing ALD processes, due to their high aspect ratio. It is worth mentioning that free-standing nanowires with extreme aspect ratios >>100:1 can vibrate, making analysis difficult. All depositions were found to result in the same thickness and

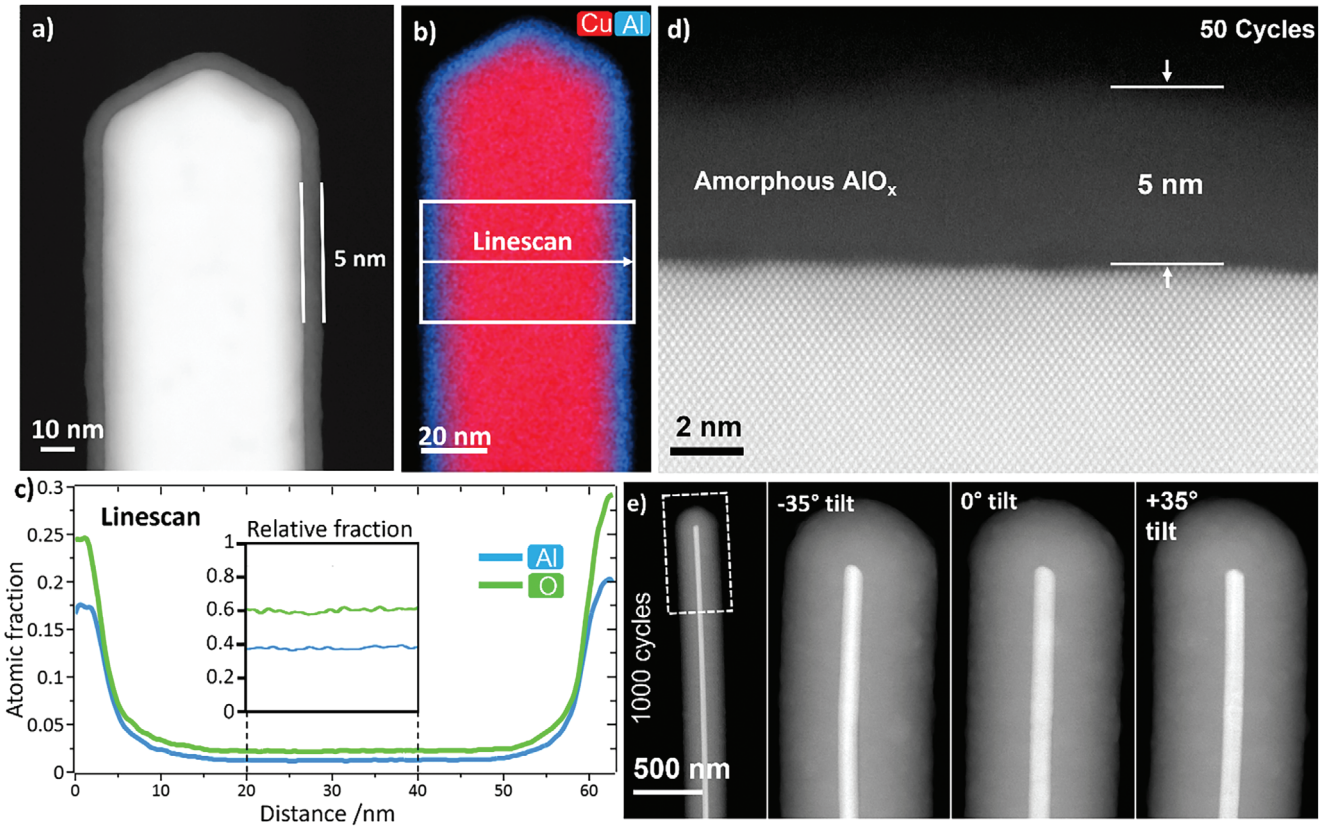

Figure 2. Characteristics of ALD layers analyzed using nanowires and TEM. a) HAADF STEM image showing the tip of a nanowire and a conformal coating of 5 nm. b) EDX map showing copper and aluminum signals. c) EDX linescan showing a continuous signal for Al and O along the wire and relative composition of 2:3 (see inset). d) High-resolution image of the edge of a nanowire showing a crystalline lattice for the wire and an amorphous structure for the coating. e) Tilt series of a coated nanowire indicating a completely conformal coating.

structure near the top and bottom of the wires (see Figure S2, Supporting Information). The TEM analysis lets us determine the layer thickness, and confirm the chemical composition and structure in addition to enabling the characterization of the conformality. This in-depth analysis of the coatings is available directly after deposition without any further preparation enabling quick process control and optimization of parameters. The here-presented TEM analysis is not exhaustive, with techniques such as electron energy loss spectroscopy (EELS) or 4D-STEM enabling further insights into properties such as bond types and local crystal orientations. The quality of the results obtained from nanowires is comparable to a cross-section specimen prepared by focused ion beam (FIB) (see Figure S3 (Supporting Information) for a comparison between the two).

3. Growth Per Cycle (GPC) Analysis

With the capabilities of the analysis technique being established, we used it to rapidly optimize the process parameters for aluminum oxide deposition in our system (Swiss Cluster SC1). To do this, we started with a standard recipe given by the manufacturer for this process (120 °C, 12 000 ms TMA-purge, 500 ms TMA-pulse, 18 000 ms water-purge, 250 ms water-pulse, 50 cycles) and then from that varied number of cycles, temperature, pulse and purge times for both precursors. In total 35 processes with variations of the parameters were run, with each process being characterized in TEM using nanowire templates immediately after deposition.

At first, we varied the cycle number to confirm the growth rate of the process (see **Figure** 3a,b). For each sample the thickness was measured using imaging and EDX maps were acquired to confirm the chemical composition. High-resolution images were acquired for low cycle numbers to get an accurate measurement of the thickness. After a single cycle, there is already a layer of ≈0.8 nm present (see Figure 3c) which grows on top of a layer of native copper oxide of a copper nanowire. This layer is not uniform in contrast, indicating an incomplete coverage of the surface. After two and three cycles (Figure 3d,e) the thickness of this layer barely increases. However, after three cycles brighter regions appear in the deposited layer (marked with arrows in Figure 3e), indicating densification. Between 10 and 50 cycles the linear growth regime with a growth per cycle of 1 Å starts which continues up to our limit of 1000 cycles. EDX maps (Figure 3b) confirm that the deposition is indeed stoichiometric aluminum oxide for all different numbers of cycles. The ratio of aluminum to oxygen stays fairly constant throughout the process. The obtained growth per cycle indicates that the standard recipe does indeed operate inside the parameter window for the TMA/water process but some of the parameters might not be optimal for the fastest deposition.

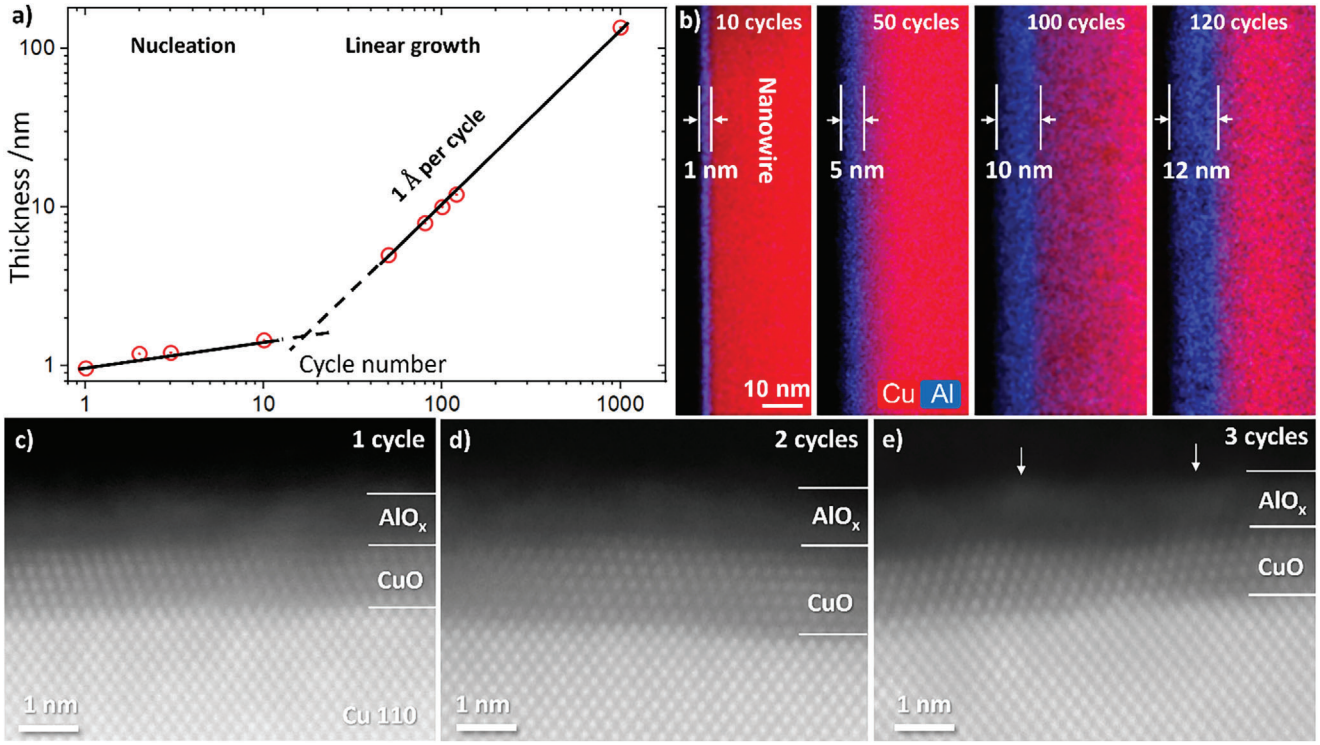

Figure 3. Thickness in dependence of cycle number for the aluminum oxide ALD process at 120 °C. a) Graph of the thickness versus cycle number showing an initial slower growth regime followed by a linear growth regime. b) EDX maps of Cu and Al showing the thickness and chemical composition for different cycle numbers. c–e) High-resolution images after deposition of 1, 2, and 3 cycles of aluminum oxide.

4. Process Optimization

With the growth per cycle for the standard process being established, we focused on optimizing different process parameters. One important parameter for the ALD process window is temperature.[34] If the temperature is too low, the ALD reaction can occur at a reduced rate due to the lack of energy and unreacted educts may be incorporated into the layer.[35] Conversely, if a temperature above the optimum is chosen, desorption of educts may increase so that the overall deposition rate is lowered. At the same time, unwanted side reactions may occur that lead to the deposition of different stoichiometries at increased rates, resulting in a higher roughness.[36] We used our method to characterize the temperature range for ALD deposition in our system by looking at the growth per cycle (for 50 cycles) at 9 different temperatures (see **Figure** 4a). In the temperature range between 120 and 200 °C we found the highest growth rate of ≈1 Å per cycle for the TMA/water process. Below that range, we see a linear decrease in the growth per cycle down to 0.56 Å per cycle at room temperature. While in typical applications this is not desirable, for some substrates lowering the temperature may be necessary. Using TEM, we can confirm that the material deposited at low temperatures has a similar structure and aluminum-to-oxygen ratio as that deposited at higher temperatures (notwithstanding a potential increase in hydrogen at low temperatures).[35] At a temperature >200 °C we also observe a linear decrease of the deposition rate down to 0.77 Å per cycle at 300 °C. This indicates increased desorption of educts before they can react with the other educt in the next step of the process. Nevertheless, the film that is deposited shows a similar structure and chemistry as the ones deposited at optimal conditions.

Depositing thick layers with a standard process is time-consuming (in our case using a standard recipe it takes ≈32 min to deposit 5 nm) and limits the application of ALD in many cases. Therefore, we varied the pulsing and purging times for both precursors of our process to optimize for the fastest possible deposition in our instrument. Pulse times refer to the time that a precursor is let into the reaction chamber whereas purging refers to the time spent to remove residual precursor molecules. We started by optimizing water (18 000 ms standard) and TMA (12 000 ms standard) purge times. If the purge time is too low, the educt has not entirely been flushed out of the chamber before the next educt is let into it. This leads to gas-phase reactions and deposition conditions resembling more a conventional CVD-type process.[37] On the other hand, if the purge times are too long, the reaction is clean and self-limiting, however, the overall deposition rate is much lower, and process times are much longer. The necessary purge times need to be individually optimized for each precursor, to account for the differences in volatility. In this study, we started from our standard process at 120 °C and varied the purge times for TMA from 500 ms to 40 s. For water, we went from 1 to 32 s (see Figure 4b). For each of these processes, a TEM analysis of the coated nanowires was performed including a characterization of the structure and chemistry of the coatings. For TMA we find a slight increase in deposition rate at purge times <1 s. For water, an increase in growth per cycle can be already noticed at purge times <6 s. At 2 s purge time, we find a growth per cycle of >1.1 Å per cycle which grows to 1.4 Å per cycle at

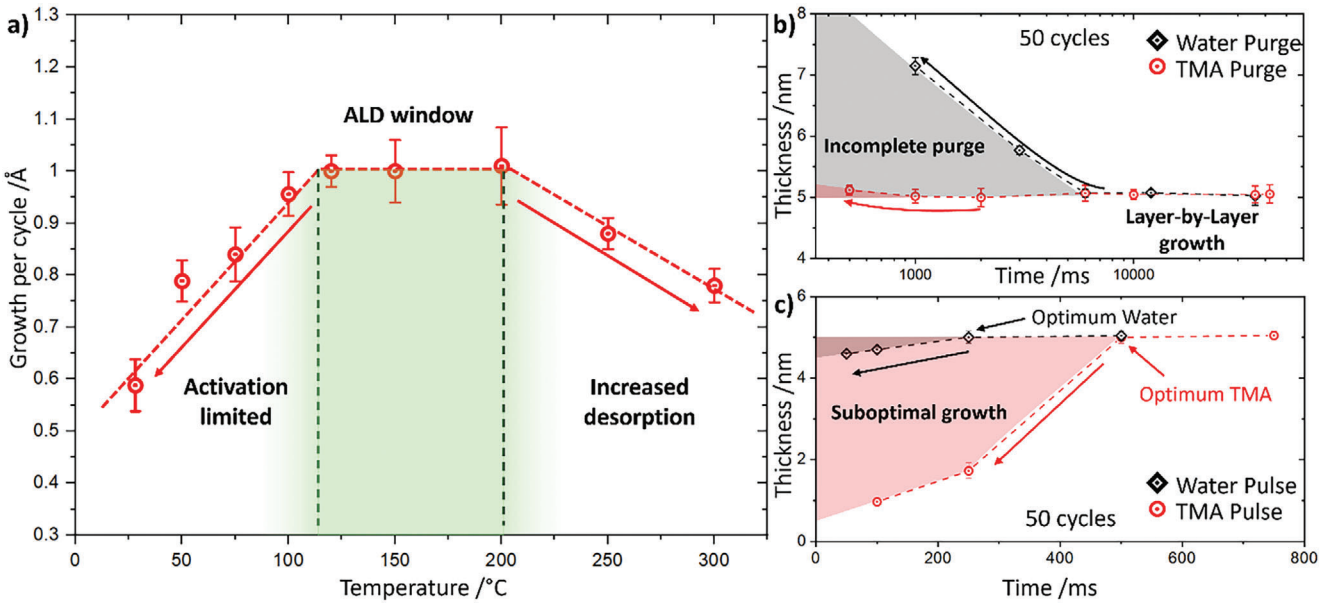

Figure 4. Temperature, pulse, and purge time optimization. a) Growth per cycle in dependence on temperature, showing an optimal plateau between 120 and 200 °C. Outside that temperature range, the GPC is reduced. b) Variation of purging times for both water and TMA. c) Optimization of pulse times, showing a lowering of the growth rate with decreasing times. Both b and c) have been performed at 120 °C.

1 s purge time. With these parameters, we can expect a crossover into a gas-phase reaction regime. Conversely, any purge time >6 s simply increases the overall process time without changing anything about the deposited material itself. We can thus conclude that for our specific reactor setup, the optimum purge times are 1 s for TMA and 6 s for water.

In the same way, the pulse times can be optimized for the two precursors (see Figure 4c). Starting with TMA we varied the pulse times from 100 to 750 ms. We found that <500 ms we see a decrease in the deposition rate to 0.3 Å per cycle at 250 ms and to <0.1 Å per cycle at 100 ms. This means there is not enough time for sufficient precursor molecules to flow into the reaction chamber and reach the sample to form a complete layer. Going in the other direction, increasing the pulse time to 750 ms did not change the process beyond the 500 ms benchmark. For water, we varied the pulse times from 50 up to 500 ms. Here the optimal pulse time is 250 ms with a growth of 1 Å per cycle. Going below that leads to a reduced deposition rate down to 0.9 Å per cycle at 50 ms pulse time. Overall, we find optimized parameters for purge times (1 s TMA, 6 s water) and pulse times (500 ms TMA, 250 ms water) that let us cut down the deposition times by a factor of almost 5. To deposit 5 nm using the non-optimized recipe takes 31:39 min compared to 6:44 min for the optimized approach. This allows us to increase layer thicknesses dramatically for a given time frame, enabling even µm sized films to be deposited in a reasonable time.

5. Discussion

ALD works well on nanowires as substrate. We tested both copper and gold as substrates and did not see significant differences between the two materials when it came to the outcome of the deposition after at least 50 cycles. Commercial silver wires showed the same outcome as the other wires that were tested. The accuracy of the thickness measurement of the ALD layers mainly depends on the resolution and calibration of the microscope used for analysis. If atomic resolution is available, the lattice spacing of the nanowire can even be used as a built-in way of calibration.

While our technique is primarily aimed at providing a way of rapidly optimizing ALD processes for a given reactor or reaction, we can also make some general observations about the TMA/water process we used. First of all, we observe that during the first few cycles of the process, the layer growth is slower than in the later stages of the process. This effect is typically attributed to an initial nucleation phase in which material only attaches to select locations onto the substrate.[29,38] Interestingly, we find the layer thickness of the deposited material after a single cycle already to be in the range of 0.8 nm which may be attributed to surface roughness and projection effects. After a second and third cycle this thickness barely increases, indicating that rather than a complete layer-by-layer growth, we see a substrate inhibited growth in these early stages of the process. It is noteworthy that after three cycles we see the beginning of what appears to be densification in the outer shell of the ALD deposition. This could mean that there is a persistent, slightly less dense layer at the interface. One indication for this is the effect of delamination which has been observed on metal wires in a previous study.[24] After increasing the cycle number, a linear growth rate of ≈1 Å can be observed from at least 50 up to our limit of 1000 cycles. For the temperature dependency, we observe an optimal window between 120 and 200 °C in which the deposition rate is highest. Below that temperature an incomplete reaction has been proposed[39] leading to lower deposition rates. Above 200 °C there is increased desorption of educts leading to incomplete reactions in each ALD cycle.

Looking at the pulse and purge times, we see similar trends for water and TMA. There is a threshold time for purging for both precursors, below which there is an increase in deposition rate.

This may be attributed to residual precursor molecules remaining in the process chamber which can directly react with the other precursor in the gas phase, leading to a combined ALD and gas phase process. Water needs substantially higher purge times (6 s compared to 1 s for TMA) which can be explained by the "stickiness" of water which is a general issue in vacuum systems.[40] For pulse times we see the opposite effect, wherein a shorter time leads to a lower deposition rate. This can be explained by the lack of precursors in the chamber during each process cycle which leads to an incomplete saturation of the surface. In this case, TMA requires longer pulse times compared to water due to its higher molecular mass and therefore slower effusion.[41] We must stress here that these absolute numbers are reactor-specific, and that care has to be taken with the position of the samples inside the reactor. Samples near the gas/pump outlets in the ALD chamber will show different optimal times than samples placed far away from these outlets.[42]

6. Conclusion

In summary, we demonstrated an accessible approach for process optimization in ALD reactors using nanowires and TEM. The use of TEM-ready high-aspect ratio templates allows for a fast analysis of process parameters and hence a quick feedback loop. In addition, the use of TEM means that the deposition of a comparably thin layer is sufficient to characterize the parameters of a deposition. TEM also enables the characterization of structure, conformality, crystallinity, chemical composition, and even bond character which makes it an ideal choice for ALD. The characterization method is more accessible than ever with modern SEMs in transmission reaching resolutions <1 nm making the approach available for many labs. Looking at the aluminum oxide process (based on TMA and water) more closely we demonstrated how the presented process control enables rapid optimization of the process, reducing processing times by a factor of 5. At the same time, the method allowed us to study the early stages of the reaction using high-resolution imaging. Here, we saw a non-uniform growth in the first few cycles, with the linear growth of the layer properly starting between 10 and 50 cycles. Our method allowed us to determine the optimal temperature window as well as pump and purge times for this process and our reactor. Overall, we are confident that this work will be a great foundation for the development of novel ALD processes and optimization of existing ones. We also think this method can be adapted to other conformal deposition techniques, such as electrodeposition or certain CVD processes, and could be exploited for correlative analyses using APT.

7. Experimental Section

Nanowire Growth: Metallic nanowires were grown via sputtering at elevated temperatures using a QPrep500 deposition system (Mantis Deposition Ltd, UK). The substrate table was heated to 650 °C and the target metal (copper or gold) was sputtered with a rate of 0.8 nm min^{-1} up to a nominal layer thickness of 200 nm. TEM folding grids (Ted Pella Inc., USA) were used as growth substrates. Commercial silver nanowires with a diameter in the range of 60 nm were acquired from Sigma Aldrich.

Atomic Layer Deposition: Aluminum oxide was deposited using TMA and water in a Swiss Cluster SC-1 instrument using only the ALD module of the deposition chamber. The reactor was connected to an EV-S50P dry pump (Ebara) presenting a pumping speed of 5000 L min^{-1} and enabling a background pressure of 2×10^{-3} mbar. The ALD parameters are described in detail in the main text.

Transmission Electron Microscopy: TEM was performed using a probe-corrected Thermo Scientific Titan Themis 200 G3 at 200 keV. Energy dispersive X-ray spectroscopy maps were acquired using the built-in SuperX detector. Sample tilting was performed using a standard Thermo Scientific double tilt holder.

Supporting Information

Supporting Information is available from the Wiley Online Library or from the author.

Acknowledgements

The authors would like to acknowledge help from Swiss Cluster AG.

Conflict of Interest

The authors declare no conflict of interest.

Data Availability Statement

The data that support the findings of this study are available from the corresponding author upon reasonable request.

Keywords

atomic layer deposition, electron microscopy, nanowires

Received: December 20, 2023
Revised: January 25, 2024
Published online:

[1] J. W. Elam, D. Routkevitch, P. P. Mardilovich, S. M. George, *Chem. Mater.* **2003**, *15*, 3507.
[2] S. M. George, *Chem. Rev.* **2010**, *110*, 111.
[3] M. Leskelä, M. Ritala, *Angew. Chem., Int. Ed.* **2003**, *42*, 5548.
[4] B. Díaz, E. Härkönen, J. Światowska, V. Maurice, A. Seyeux, P. Marcus, M. Ritala, *Corros. Sci.* **2011**, *53*, 2168.
[5] A. C. Dillon, A. W. Ott, J. D. Way, S. M. George, *Surf. Sci.* **1995**, *322*, 230.
[6] E. Guziewicz, T. A. Krajewski, E. Przezdziecka, K. P. Korona, N. Czechowski, L. Klopotowski, P. Terziyska, *physica status solidi* **2020**, *257*, 1900472.
[7] X. Meng, Y.-C. Byun, H. S. Kim, J. S. Lee, A. T. Lucero, L. Cheng, J. Kim, *Materials* **2016**, *9*, 1007.
[8] H. Kim, *J. Vac. Sci. Technol.* **2003**, *21*, 2231.
[9] B. S. Lim, A. Rahtu, R. G. Gordon, *Nat. Mater.* **2003**, *2*, 749.
[10] M. B. E. Griffiths, P. J. Pallister, D. J. Mandia, S. T. Barry, *Chem. Mater.* **2016**, *28*, 44.
[11] H. H. Sønsteby, A. Yanguas-Gil, J. W. Elam, *J. Vac. Sci. Technol.* **2020**, *38*, 020804.
[12] A. Yanguas-Gil, J. W. Elam, *J. Vac. Sci. Technol.* **2011**, *30*, 01A159.
[13] S. W. Lee, B. J. Choi, T. Eom, J. H. Han, S. K. Kim, S. J. Song, W. Lee, C. S. Hwang, *Coord. Chem. Rev.* **2013**, *257*, 3154.

[14] B. S. Lim, A. Rahtu, J.-S. Park, R. G. Gordon, *Inorg. Chem.* **2003**, *42*, 7951.
[15] S. Ferrari, M. Modreanu, G. Scarel, M. Fanciulli, *Thin Solid Films* **2004**, *450*, 124.
[16] B. B. Burton, D. N. Goldstein, S. M. George, *J. Phys. Chem. C* **2009**, *113*, 1939.
[17] D. R. G. Mitchell, D. J. Attard, G. Triani, *Thin Solid Films* **2003**, *441*, 85.
[18] I. Iatsunskyi, G. Gottardi, V. Micheli, R. Canteri, E. Coy, M. Bechelany, *Appl. Surf. Sci.* **2021**, *542*, 148603.
[19] D. N. Goldstein, J. A. McCormick, S. M. George, *J. Phys. Chem. C* **2008**, *112*, 19530.
[20] H. Fukuzawa, H. Yuasa, H. Iwasaki, *J. Phys. D: Appl. Phys.* **2007**, *40*, 1213.
[21] Y. Wu, A. D. Giddings, M. A. Verheijen, B. Macco, T. J. Prosa, D. J. Larson, F. Roozeboom, W. M. M. Kessels, *Chem. Mater.* **2018**, *30*, 1209.
[22] L. A. Giannuzzi, F. A. Stevie, *Micron* **1999**, *30*, 197.
[23] L. D. Madsen, L. Weaver, S. N. Jacobsen, *Microsc. Res. Tech.* **1997**, *36*, 354.
[24] L. M. Vogl, P. Schweizer, L. Pethö, A. Sharma, J. Michler, I. Utke, *Nanoscale* **2023**, *15*, 9477.
[25] L. M. Vogl, P. Schweizer, P. Denninger, G. Richter, E. Spiecker, *ACS Nano* **2022**, *16*, 18110.
[26] Y. Wang, V. Schmidt, S. Senz, U. Gösele, *Nat. Nanotechnol.* **2006**, *1*, 186.
[27] L. M. Vogl, P. Schweizer, M. Wu, E. Spiecker, *Nanoscale* **2019**, *11*, 11687.
[28] L. M. Vogl, P. Schweizer, G. Richter, E. Spiecker, *MRS Adv.* **2021**, *6*, 665.
[29] R. L. Puurunen, *J. Appl. Phys.* **2005**, *97*, 121301.
[30] K. W. Urban, *Science* **2008**, *321*, 506.
[31] P. Schweizer, C. Dolle, E. Spiecker, *Sci. Adv.* **2018**, *4*, eaat4712.
[32] T. Klein, E. Buhr, C. G Frase, *Advances in Imaging and Electron Physics* (Ed: P. W. Hawkes), Elsevier, Amsterdam, The Netherlands **2012**, pp. 297–356.
[33] P. Schweizer, P. Denninger, C. Dolle, E. Spiecker, *Ultramicroscopy* **2020**, *213*, 112956.
[34] R. W. Johnson, A. Hultqvist, S. F. Bent, *Mater. Today* **2014**, *17*, 236.
[35] C. Guerra-Nuñez, M. Döbeli, J. Michler, I. Utke, *Chem. Mater.* **2017**, *29*, 8690.
[36] J. Aarik, A. Aidla, H. Mändar, V. Sammelselg, *J. Cryst. Growth* **2000**, *220*, 531.
[37] H. Jain, P. Poodt, *Dalton Trans.* **2021**, *50*, 5807.
[38] R. L. Puurunen, W. Vandervorst, *J. Appl. Phys.* **2004**, *96*, 7686.
[39] M. D. Groner, F. H. Fabreguette, J. W. Elam, S. M. George, *Chem. Mater.* **2004**, *16*, 639.
[40] A. Berman, *Vacuum* **1996**, *47*, 327.
[41] E. A. Mason, B. Kronstadt, *J. Chem. Educ.* **1967**, *44*, 740.
[42] G. P. Gakis, H. Vergnes, E. Scheid, C. Vahlas, A. G. Boudouvis, B. Caussat, *Chem. Eng. Sci.* **2019**, *195*, 399.